VI Serbian-Belarusian Symp. on Phys. and Diagn. of Lab. &
Astrophys. Plasma, Belgrade, Serbia, 22 - 25 August 2006
eds. M. Ćuk, M.S. Dimitrijević, J. Purić, N. Milovanović
Publ. Astron. Obs. Belgrade No. 82 (2007), 201-211 *Invited lecture*

LASER ABLATION PLASMAS IN LIQUIDS FOR FABRICATION OF NANOSIZE PARTICLES

N.V. Tarasenko, V.S. Burakov, A.V. Butsen

Institute of Molecular and Atomic Physics National Academy of Sciences of Belarus
70 Nezalezhnasty Ave., 220072 Minsk, Belarus
e- mail: tarasenk@imaph.bas-net.by

Abstract. The capabilities of laser ablation in liquids for fabrication of metallic and composite nanoparticles were analyzed. The properties of Ag, Au and Cu as well as bimetallic Ag-Cu and Ag-Au nanoparticles synthesized in different liquids (water, acetone, ethanol) were examined.

The results obtained showed both the mean size of the nanoparticles and their stability could be controlled by proper selection of the parameters of laser ablation such as temporal delays between pulses, laser fluence and a sort of liquid used. The optimal conditions favoring the formation of nanoparticles with a desired structure were found.

1. INTRODUCTION

Last years considerable efforts have been directed to preparation and investigation of nanostructured materials. Broadly defined, nanostructured materials are solids composed of structural elements (mostly crystallites) which characteristic size falls in the range of 1 – 100 nm [1]. They include nanocomposites, loosely aggregated nanoparticles, cluster-assembled materials, nanocrystalline thin films, metal colloids as well as semiconductor nanostructures such as quantum dots, wires and wells.

Due to the reduced size of their constituent elements nanostructured materials have electronic, magnetic and chemical properties, which differ considerably from those of the corresponding bulk materials. For example, nanostructured materials have been found to exhibit increased strength and hardness, higher electrical resistivity, enhanced diffusivity, reduced density, etc. compared to the bulk. Hence, these materials are promising candidates for a variety of applications, which include heterogeneous catalysis, gas sensor technology, microelectronics, nonlinear optics, etc. [2-4].

Depending on the size range, shape and chemical composition of nanoparticles different techniques have been used for producing of such samples. Among them are wet chemical processes, physical methods and combined techniques [5-7]. The ultimate goal of each technique is a fabrication of monodisperse particles with a predetermined size and shape.

Recently, plasma assisted methods based on laser ablation and electrical discharges have become a focus of many studies [8-11]. The capabilities of laser ablation technique and the results of its application for fabrication of metallic and composite nanoparticles are discussed in the present paper.

Laser ablation plasma is formed above the surface of the solid target when an intense laser beam strikes the target. Laser ablation provides a simple and contaminant-free method which can be used for a large number of materials. The important advantages of laser ablation technique are:

- laser ablation can be used for metals, semiconductors and insulators,
- conditions during the laser ablation can be fairly well controlled,
- in the case of multi – component samples, the stoichiometry of the ablated material can be achieved to closely resemble that of the target.

Typically, laser ablation experiments are carried out in gas or vacuum environments. The technique allows changing the diameter of nanoparticles by means of changing the energy of laser radiation, sort and pressure of an ambient gas. But efficiency of this technique is not very high in result of material depositions on walls of the vacuum chamber.

The more effective collection of synthesized particles can be achieved by laser ablation in liquid environment. Additional advantage of this approach - experiments are performed at the normal atmosphere.

It should be noted that the processes of laser ablation in liquids have been much less investigated. But the feasibility of using laser ablation in transparent liquids for nanoparticle synthesis has been recently demonstrated [8-10].

We developed the double-pulse laser ablation approach in liquid environment for fabrication of metallic and bimetallic nanoparticles with a controlled size distribution. Double-pulse approach of laser ablation has been recently shown to enhance considerably the line emission from the plume that is highly important for improvement of sensitivity of laser spectral analysis (LIBS) [12-15]. As concerns of the nanoparticles formation, the double-pulse laser ablation seems to be also more favorable than single pulse regime. The developed technique offers the better control over the particle formation process. The definite size reduction of particles in ablation plume can be achieved under conditions of suitable temporal delays between two laser pulses in result of heating and fragmentation of the ablated material produced by the first laser pulse [16].

2. EXPERIMENTAL

Experiments were made by using two 10 Hz pulsed Nd:YAG lasers, operating at the fundamental (1064 nm) and frequency-doubled (532 nm) wavelengths each with 50 mJ pulse in a 5-mm beam. The laser beams were focused on the surface of the metallic sample (Ag, Cu, Au) or combined target consisted of two tightly pressed (silver/copper or silver/gold) plates immersed into the cell with liquid. In the case of the combined target the laser beams were focused on the Ag-Cu or Ag-Au interface. Laser beams were employed for ablation both singly and together with appropriate temporal delays between pulses. The ablation laser power densities at the target surface were in the range of $5 \cdot 10^8$ - $5 \cdot 10^9$ W/cm^2. Experiments were performed using different liquids like acetone, ethanol, and distilled water.

We used two different laser beam configurations: (1) the double-pulse approach based on collinear beams focused onto the same place of the target surface and (2) the configuration based on crossed beams when the second unfocused laser beam at λ=532 nm runs parallel to the sample surface, providing additional irradiation of the formed nanoparticles.

The fabricated nanoparticles were characterized by optical absorption spectroscopy for monitoring the changes in the plasmon absorption characteristics, transmission electron microscopy (TEM), X-ray diffraction (XRD) and energy dispersive X-ray microanalysis (EDX) in order to analyze the final size and composition of nanoparticles.

3. RESULTS AND DISCUSSION

Two main mechanisms of nanoparticle formation during laser ablation process can be distinguished.

- The first mechanism, associated with aggregation of the ablated atoms and clusters into small embryonic nanoparticles and their growth by assembling the clusters and attachment of free atoms.
- The second one, attributed to the plasma-induced heating and ablation of particulates from the target.

According to the first mechanism the density of ablated species (atoms) in the gas phase plays an important role in the nanoparticles growth. By controlling the density of the ablated species it is possible to control the final size of the formed nanoparticles. The density of the ablated species can be changed by adjusting the laser fluence. It should be noted that the second mechanism gives rise to much larger particle sizes and broader size distributions.

Relative contributions of the both mechanisms determine the final size distribution of the produced particles. That’s why for optimization of synthesis process the detailed information about plasma parameters is required.

Spectroscopic characterization of the ablated plume was performed by the time resolved emission spectroscopy and gated intensified CCD imaging technique (Fig.1).

The optical observation of the plasma emission was executed by imaging the plasma plume onto the entrance slit of the spectrograph such that the expansion direction (z) lies along the orientation of the entrance slit of the spectrograph. At the output of the spectrograph, in the image plane, a time-gated ICCD camera was installed. So, at its output the spectrograph produced a one-dimensional spatial and spectral image of the expanding plasma, in which the vertical axis corresponds to the expansion direction z and the horizontal axis to the wavelength of the emission of plasma species.

The emission spectrum was recorded at different time delays. Typical gate steps and gate widths used were 100 and 50 ns, respectively, which were selected in order to give the optimal signal/amplitude ratio and temporal resolution.

Plasma emission spectra were recorded and compared for different ablation regimes (single pulse, two pulses in coincidence and in sequence at various delays between pulses).

Summarizing the results of our investigations and results of previous studies of double-pulse laser ablation plasma for spectral analysis [15,17], the main features of double-pulse laser ablation in liquids can be characterized as following:

- A hemispherical cavitation bubble originated from gaseous ablation products is formed above the sample.
- Arising after the ablating pulse and expanding steadily, the bubble reaches its maximum size after several tens of microseconds (depending on the sample material and laser fluence) and then collapses.
- The dimension of laser ablation plasma in liquid is significantly smaller, vertically and horizontally, than the plume produced in air. For illustration Fig.2 presents intensity profiles in the direction of the normal to the sample surface for emission from the 1064-532 nm double-pulse laser-induced plasma of a copper sample (z = 0 mm), obtained under air and water environment.
- Plasma radiation after single-pulse ablation is weaker (compared to gaseous environments) because it is strongly quenched. The spectrum of the plume is dominated by continuum radiation.
- But from double-pulse ablation plasma sharp atomic line spectra were observed. The Fig. 2B presents the fragments of the spectra of the laser-induced plasma of a copper sample in case of the 532 nm single (A) and in the 1064-532 nm double-pulse ablation modes for gate delays with respect to the 532 nm laser 200 (b), 400 (c) and 600 ns (d). The mechanism responsible for the distinct line excitation produced by the second pulse has been attributed to the formation of a bubble at the surface by the first laser pulse. The second pulse fired into the bubble under gaseous environments. The optimal values of pulse separations are determined by larger bubble volume that leads to increase the emission intensity and to decrease quenching of emitting atoms.

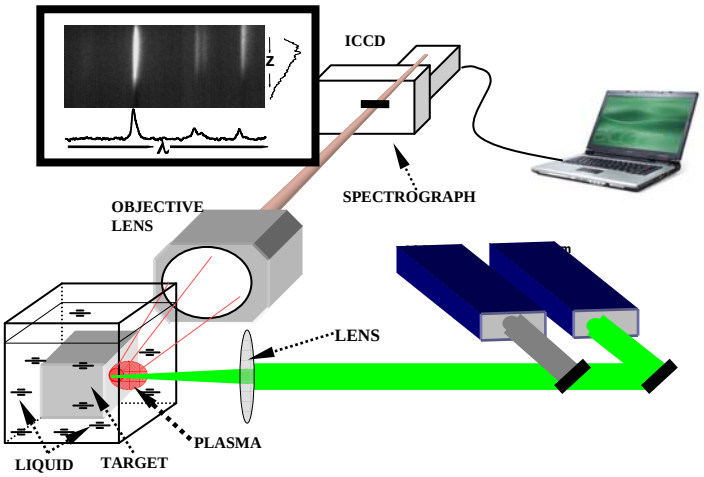

Fig.1. Experimental set-up for time-resolved spectroscopic plasma characterization.

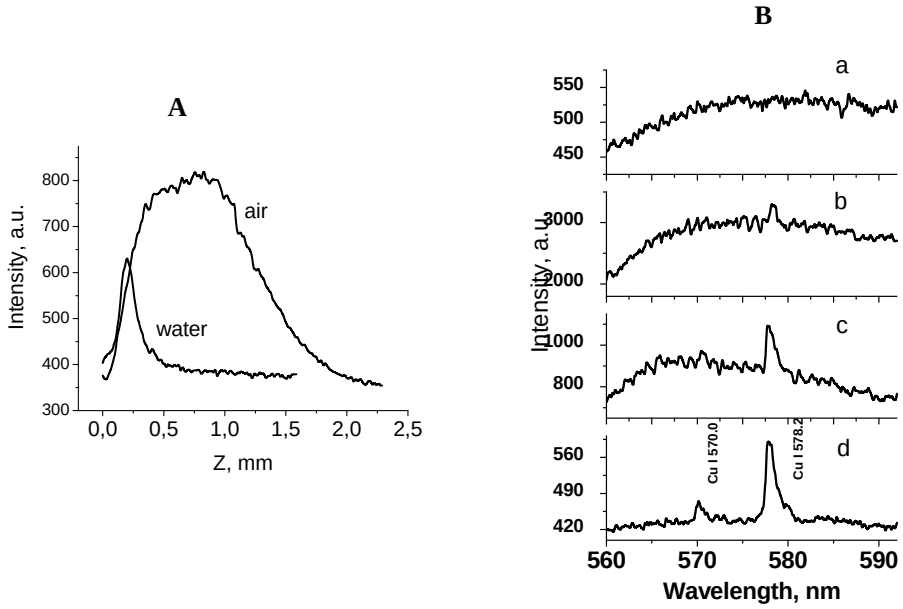

Fig.2. A - Intensity profiles in the direction of the normal to the sample surface for emission from the 1064-532 nm double-pulse laser-induced plasma of a copper sample (z = 0 mm), obtained under air and water environment; **B -** fragments of the spectra of the laser-induced plasma of copper sample in case of the 532 nm single (a) and in the 1064-532 nm double-pulse ablation mode for gate delays with respect to the 532 nm laser 200 (b), 400 (c) and 600 ns (d).

During the repeated (10 Hz) laser ablation of the metal samples the solution in the cell became visibly contaminated with the ablated material. The properties of metal nanoparticles fabricated by laser ablation were studied by recording their extinction spectra as a function of preparation conditions. Typical spectra of the prepared colloids are shown in Fig.3 and Fig.4. The spectra exhibit characteristic absorption bands with peaks located at 400 nm for silver nanoparticles and at 520 nm for gold nanoparticles. The spectral features of copper colloids are characterized by a peak of absorbance at 570 nm (Fig.4).

These bands were clearly seen in all solutions and they are related to the collective excitation of conduction electrons (surface plasmon resonances SPR). The position and shape of the plasmon absorption are known to be dependent on the particle morphology, dielectric functions of the metal and the surrounding medium as well as surface-absorbed species [1]. The presence of the single surface-plasmon peaks implied that the formed nanoparticles were nearly spherical. In the case of ellipsoidal particles the absorption spectrum would have two plasmon peaks [18].

According to Mie theory spectra of the particles with radii between about 2 and 10 nm are independent of the particle size. For particles with dimensions beyond 10 nm the absorption peak broadens and shifts to longer wavelength. The broadening and lowering of the absorption peak can be related to a reduced mean free path for conduction electrons. The peak position at 400 nm observed for silver in our experiments indicated a formation of Ag nanoparticles with sizes in the range of 10 –30 nm.

Gold colloids exhibit the characteristic peaks of the surface plasmon resonance (SPR) on the tail of the broad band extending toward the UV- wavelength range and originating from the interband transitions of gold nanoparticles [19]. It is known that the absorption due to the interband transition does not change appreciably with the particle size but is sensitive to the particle quantity.

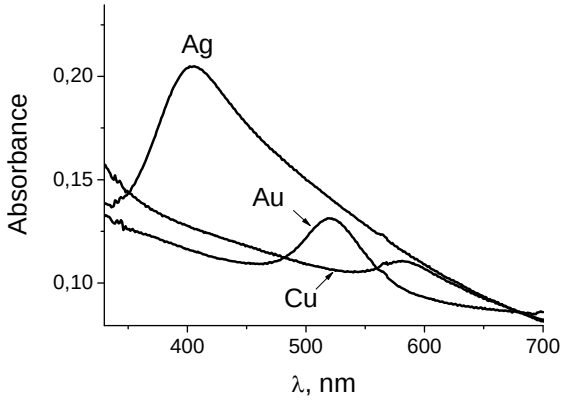

Fig.3. Extinction spectra of silver, gold and copper colloids prepared by laser ablation in ethanol.

Therefore, the absorption of the solution at the wavelengths of interband transitions can be used as a measure of the total amount of gold in the solution including the nanoparticles of different sizes, clusters and free gold atoms. Conversely, the height of the plasmon peak is proportional to the concentration of the Au nanoparticles with sizes in the range of 5 – 30 nm. The absorbance in the vicinity of 200 nm can be assigned to the small gold clusters, which begin to contribute to the optical absorption in the range of the surface plasmon resonance as they grow into nanosized particles, by aggregation and attachment processes [20].

Analogous considerations can be made for the absorption spectra of copper nanoparticles. In this case the size effect is similar to that of gold. At very small sizes limitation of the mean free path by the particle boundary broadens and decreases peak absorption, while at larger sizes the peak shifts to longer wavelengths and broadens as high order modes are excited. For example, the copper particles with a diameter below 4 nm are characterized by such a strong broadening of the plasmon resonance that it practically disappeared [21]. A progressive appearance of the peak at 570 nm occurs upon increasing the size of the copper nanoparticles.

Owing to the high reactivity of copper, it was practically impossible to observe the copper plasmon band near 570 nm by laser ablation in water. But Cu nanoparticles with the average diameter of 5-7 nm exhibiting the characteristic plasmon band were synthesized by laser ablation of a copper metal plate immersed in the aqueous solution of sodium dodecyl sulfate (SDS) [22].

In our experiments [16] the shape and intensity of the plasmon bands in the absorption spectra of colloidal solutions were also dependent on the regime of laser operation (double-pulse or single pulse mode). By using the double pulse laser ablation and the same total number of laser pulses, the efficiency of ablation was greater and the absorption bands were more intense. The observed spectra were also changed with changing of the temporal delay between two pulses in double pulse mode. It should be noted that particles prepared by the double-pulse laser ablation had smaller diameters than those prepared in the single pulse ablation regime. The size reduction of particles in ablation plume is most likely to achieve under conditions of suitable temporal delays in result of heating and fragmentation of the ablated material produced by the first laser.

It is important to mention that the particles produced in acetone show a long-term stability towards coagulation/aggregation as compared to that in water. This function of acetone most probably is connected with the interaction between the acetone carbonic group and the metal nanoparticle surface.

The spectra findings were confirmed by TEM data. The size and size distribution of the nanoparticles were found to be functions of the laser ablation parameters (laser wavelength and fluence). Typical TEM images and histograms of the diameter distributions for Cu nanoparticles synthesized by the 532 nm laser ablation in acetone are presented in Fig.4. TEM images show the presence of nearly spherical particles with an average diameter of 10±2 nm.

The TEM of the Ag particles fabricated by laser ablation indicated that the average size of the particles was around 15 nm with an asymmetrical distribution of sizes ranging from approximately 5 to 35 nm. The average size of gold

nanoparticles, formed at the same experimental conditions was about 15 nm. The average diameter was found to be decreased as the laser fluence increased. Some of the nanoparticles were loosely agglomerated, some presented chains of welded particles.

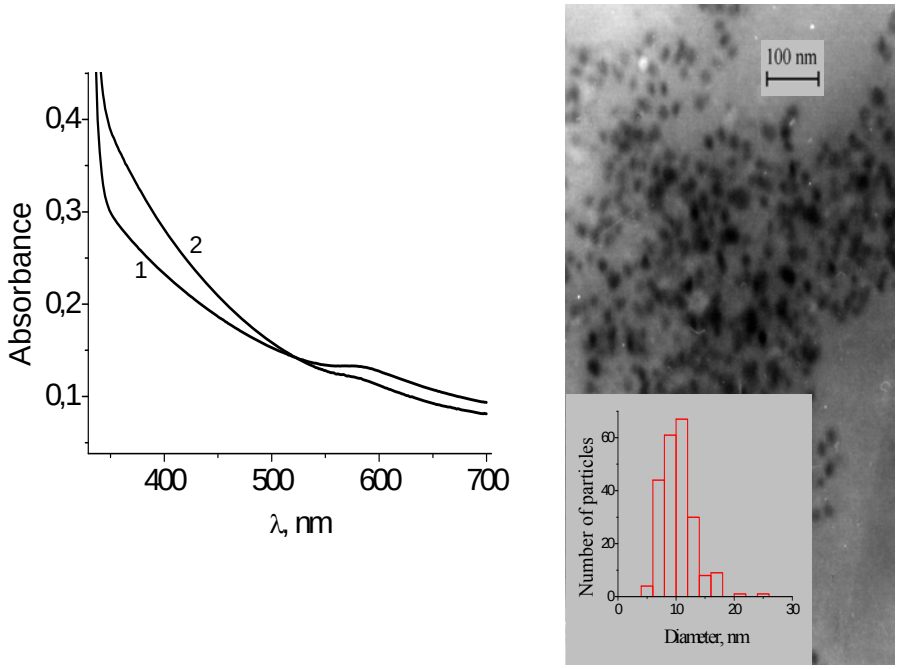

Fig. 4. Extinction spectra of copper nanoparticles prepared in acetone: (1) by the repetitive (10Hz) 1064 nm single-pulse laser ablation for 5min; (2) by the double-pulse laser ablation (10 μs separation between the 1064nm and 532 nm pulses) (**left**) and TEM image with corresponding size distribution histogram of Cu nanoparticles prepared in single pulse regime in acetone (**right**).

In the case of combined target consisted of two tightly pressed silver/copper or silver/gold plates immersed into the cell with acetone when the laser beams focused on the Ag-Cu or Ag-Au interface, the spectra of the solutions do not exhibited a pronounced maximum attributable to the monometallic particles. These spectra showed a single SPR whose position was dependent on a ratio of element concentrations, which can be changed by the variation of the ratio of the irradiated areas of both metals in the focal plane of a lens focusing the laser radiation on the target surface. It should be noted, that the absorption curve of the bimetallic dispersion could not be obtained by simple overlapping of the absorption curves of the monometallic Ag and Cu (Au) particles. Two separate maxima that correspond to the plasmon bands of individual metals should be observed in case of a mixture of monometallic particles or bimetallic particles of a core-shell structure. Therefore

based on the spectra analysis, it is reasonable to conclude that bimetallic (composite) nanoparticles are formed. It is known that silver and copper exhibit very limited miscibility in the bulk, while gold and silver are completely miscible. Therefore, most likely in case of Ag-Cu target, the silver/copper particles are phase-separated composites, which are made partly of silver and partly of copper atoms and in the case of Ag-Au sample a formation of alloys is preferable.

EDXS and XRD analysis also pointed to the bimetallic composition of the formed nanoparticles. Scanning electron micrographs when viewed with greater magnification showed that the rather large grains formed after deposition of the colloidal solution onto silicon substrate were seen to be clusters of many smaller grains (Fig.5). The EDX spectra showed the presence of both constituent elements along the line of scanning. XRD analysis of the produced powders showed that the characteristic peaks for a Ag–Cu bimetallic system became broader and accordingly suggested the formation of bimetallic nanoparticles with smaller sizes.

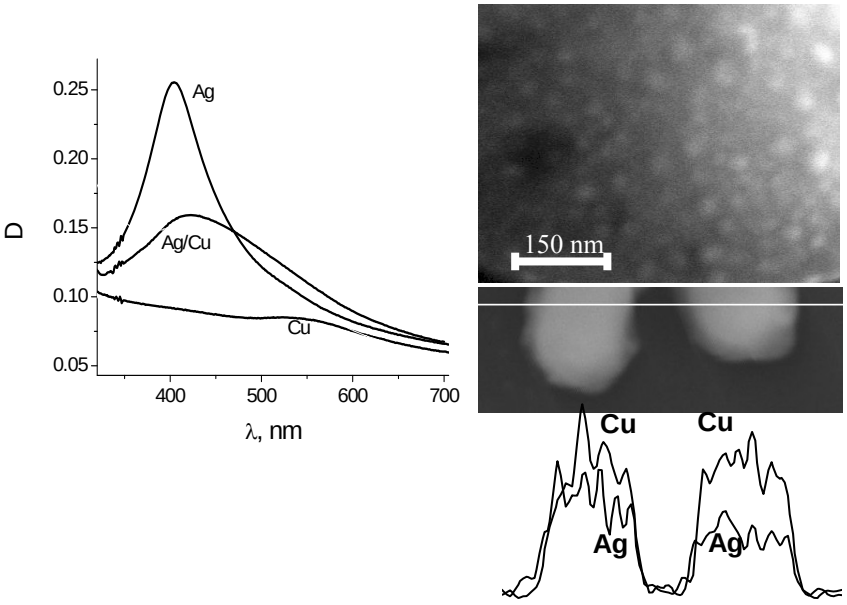

Fig. 5. Extinction spectra of silver, copper and bimetallic silver/copper colloids prepared by single-pulse laser ablation **(left)** and SEM images of bimetallic Ag-Cu nanoparticles with distribution of elements along the line of scanning measured by EDX **(right).**

TEM data confirmed that the laser ablation of the combined target produced the particles of smaller (5-7 nm) sizes than the particles formed under the laser ablation of the monometallic samples. From the diffractions patterns, it was revealed that the individual particles were polycrystalline.

It is important to note that bimetallic nanoparticles, are even of greater interest than the monometallic ones because of their composition-dependent optical and catalytic properties. For example, the enhanced catalytic performance of bimetallic nanoparticles compared with the single metal ones is well established [23,24].

4. CONCLUSION

It is expected, that the obtained results will find applications in the synthesis of new materials with modified properties, in the fabrication of catalysts with optimized selectivity and efficiency, in medicine for preparation of nanoparticle-based probes with great potential for targeting, imaging and treating different diseases etc.

ACKNOWLEDGEMENTS

The work has been partially supported by the Belarusian Foundation for Fundamental Researches under grant F 06-094 and by the Presidium of the National Academy of Sciences under grant № 02.

REFERENCES

1. U. Kreibig, M. Vollmer, Optical Properties of Metal Clusters, Springer, Berlin (1995).
2. M.S. Sibbald, G. Chumanov, T.M. Cotton, J. Phys. Chem. **45**, 721 (1998).
3. R.A.Ganeev, A.I.Ryasnyanskii, T.Usmanov, Quantum Electronics **31**, 185 (2001)
4. J. Neddersen, G. Chumanov, T. Cotton, Appl. Spectr. **47**, 1959 (1993).
5. Ю.В. Бокшиц, Г.П. Шевченко, В.В. Свиридов, Весці НАН Беларусі, сер. хім. навук, **1**, 19 (2001).
6. Mark T.Swihart, Current Opinion in Colloid and Interface Science **8**, 127 –133 (2003).
7. C.-H. Jung, H.-G. Lee, C.-J. Kim and S.B. Bhaduri, J. of Nanoparticle Research **5**, 283-388 (2003).
8. N.V. Tarasenko, E.A. Nevar, A.V. Butsen, N.A. Savastenko, Appl. Surf. Sci., **252**, 4439-4444 (2006).
9. A. Simakin, V. Voronov, G. Shafeev, R. Brayner, F. Bozon-Verduraz, Chem. Phys. Lett. **348**, 182 (2001).
10. A.V. Kabashin, M. Meunier, C. Kingston, and John H.T. Luong, J. Phys. Chem. B **107**, 4527 (2003).
11. N. Parkansky, B. Alterkop, R.L. Boxman, S. Goldsmith, Z. Barkay, Y. Lereah, Powder Technology **150**, 36 – 41 (2005).

12. M. L. Petukh, V. A. Rozantsev, A. D. Shirokanov, A. A. Yankovskii, J. Appl. Spectr. **67**, 1097-1101 (2000).
13. S. M. Pershin, Quantum Electronics **16**, 325-330 (1989).
14. L.St-Onge, V.Detalle, M.Sabsabi, Spectrochimica. Acta B **57**, 121-135 (2002).
15. A. Pichahchy, D. Cremers, M. Ferris, Spectrochimica Acta B **52**, 25-39 (1997).
16. V.S. Burakov, N.V. Tarasenko, A.V. Butsen, V.A. Rozantsev, M.I. Nedel'ko, Eur. Phys. J. Appl. Phys. **30**, №2, 107-113 (2005).
17. R. Nyga, and W. Neu, Opt. Lett. **18**, 747-749 (1993)
18. S. Link, C. Burda, B. Nikoobakht, and M.A. El-Sayed, J. Phys. Chem. B **104**, 6152 (2000).
19. C.F. Boren, D.R. Huffman, Absorption and Scattering of Light by Small Particles, Wiley, New York, 1983.
20. F. Mafune, J. Kohno, Y. Takeda, and T. Kondow, J. Phys. Chem. B **106**, 8555 (2002).
21. M. Aslam, G. Gopakumar, T.L. Shoba, et.al. J. Colloid. Inter. Sci. **79**, 255 (2002).
22. V.S. Burakov, E.A. Nevar, P. Ya. Misakov, N.A. Savastenko, and N.V. Tarasenko, Proceedings IV International Symposium "Laser Technologies and Lasers". October 8-11, Plovdiv, Bulgaria, 277-281.
23. Chen Yu-Hung and Yeh Chen-Sheng, Chem. Commun., 371–372 (2001).
24. J.F. Sanchez-Ramirez, C. Vazquez-Lopez, U. Pal, Superficies y Vacio **15**, 16–18 (2002).